Polymer Chemistry

RSC Publishing

PAPER

View Article Online
View Journal | View Issue

Cite this: *Polym. Chem.*, 2013, **4**, 536

A thieno[3,4-*f*]isoindole-5,7-dione based copolymer for polymer solar cells†

Yue Wu,[ab] Yan Jing,[a] Xia Guo,[a] Shaoqing Zhang,[a] Maojie Zhang,[a] Lijun Huo[a] and Jianhui Hou*[a]

Received 22nd August 2012
Accepted 11th September 2012

DOI: 10.1039/c2py20674a

www.rsc.org/polymers

A new polymer based on thieno[3,4-*f*]isoindole-5,7-dione (TID) and benzo[1,2-*b*:4,5-*b*]dithiophene was designed and synthesized. The copolymer was characterized by elemental analysis, gel permeation chromatography (GPC), thermogravimetric analysis (TGA), differential scanning calorimetry (DSC), ultraviolet-visible (UV-vis) absorption spectra as well as electrochemical cyclic voltammetry (CV) tests. Compared to PBDTTPD, introducing the quinoid unit could elevate the HOMO energy level and lower the LUMO energy level of the polymer, and consequently, the band gap can be reduced very effectively. The electronic structures of the two polymers were also studied by DFT calculations at the B3LYP/6-31G level. When a polymer solar cell (PSC) device was fabricated with an active layer of a blend of PBDTTID and $PC_{61}BM$ using 3% (v/v) diiodooctane (DIO) as a solvent additive, a high V_{oc} of 0.80 V was obtained, with a PCE of 3.12% under AM 1.5G conditions. The PBDTTID-based PSC device shows a slightly lower V_{oc} but better J_{sc} and FF than the PBDTTPD-based PSC device, and the preliminary results indicate that TID will be a desirable building block for designing photovoltaic polymers with low-lying HOMO energy levels, as well as low band gaps.

Introduction

In recent years, the polymer solar cell (PSC) has attracted considerable attention for the next generation of renewable energy technology due to its potential for making low cost and light weight solar panels through roll-to-roll printing techniques.[1,2] Over the past 10 years, the power conversion efficiencies (PCEs) of PSCs have reached over 7%.[3–13] Absorption bands and molecular energy levels are two key parameters for polymer photovoltaic materials. Great efforts have been devoted to molecular design for conjugated polymers with broad absorption bands and appropriate molecular energy levels. Building a conjugated backbone with a donor–acceptor (D–A) structure has been proved to be an effective way to tune the optical properties of conjugated polymers.[14] In these polymers, electron-deficient units (acceptor units) play a very important role. By modifying the electron withdrawing effect of the acceptor unit, the band gaps and molecular energy levels of the conjugated polymers can be tuned rationally. For example, 2,1,3-benzothiadiazole (BT)[15–20] is an electron-deficient unit widely used in polymer photovoltaic materials. When BT was copolymerized with different conjugated units, the band gaps of the resulting polymers varied from 1.9 eV to 1.5 eV.[18,19]

Another effective strategy to obtain low band gap polymers is to introduce conjugated components with strong quinoid properties into the conjugated main chain. The polymers based on benzo[1,2-*b*:4,5-*b*′]dithiophene (BDT) and thieno[3,4-*b*]thiophene (TT) provide excellent examples.[3,4,9,13,20–22] The alternative copolymer of BDT and thiophene showed a band gap of 2.0 eV;[23] after introducing a fused thiophene ring on the thiophene units, a band gap of 1.5 eV could be realized.[21] Thieno[3,4-*b*]pyrazine (TPZ)[24] is another conjugated component with strong quinoid properties, and TPZ-based copolymers commonly exhibit very low band gaps. For example, the alternative copolymer of BDT and TPZ exhibited a band gap of 1.2 eV,[23] which is much lower than that of PBDTTT.

As a fused conjugated unit, thieno[3,4-*f*]isoindole-5,7-dione (TID) consists of a six-membered ring and a five-membered ring, and since the six-membered ring on TID can form a stable aromatic electron structure, as shown in Scheme 1, the quinoid structure of TID can be stabilized well.[25] In the three above mentioned conjugated components with strong quinoid properties, the photovoltaic performances of TT and TPZ-based polymers have been well investigated and quite a few works have been reported. Although TID has been found to be a useful unit to build low band gap polymers, the photovoltaic properties of TID-based polymers have been seldom reported.[26,27]

[a]*State Key Laboratory of Polymer Physics and Chemistry, Beijing National Laboratory for Molecular Sciences, Institute of Chemistry, Chinese Academy of Sciences, Beijing 100190, China*

[b]*Graduate University of Chinese Academy of Sciences, Beijing 100049. E-mail: hjhzlz@iccas.ac.cn; Tel: +86-10-82615900*

† Electronic supplementary information (ESI) available: experimental section, TGA and DSC plots, and AFM images of the pure polymer film. See DOI: 10.1039/c2py20674a

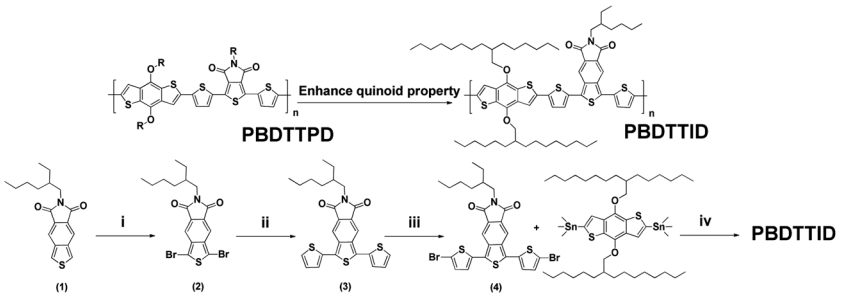

Scheme 1 The synthetic route to the polymer; (i) NBS, DMF, 0 °C, (ii) 2-trimethyl(thiophene-2-yl)stannane, $Pd(PPh_3)_4$, toluene–DMF (5 : 1), inert atmosphere reflux, 16 h; (iii) NBS, DMF, 0 °C, (iii) $Pd(PPh_3)_4$, toluene–DMF (5 : 1), inert atmosphere reflux, 16 h.

Experimental

Synthesis

Materials. (4,8-Bis((2-hexyldecyl)oxy)benzo[1,2-*b*:4,5-*b*′] dithiophene-2,6-diyl)bis(trimethylstannane) was purchased from Solarmer Materials Inc. $Pd(PPh_3)_4$ was purchased from Frontiers Scientific Inc. All of these chemicals were used as received. Tetrahydrofuran (THF) was dried over Na/benzophenone ketyl and freshly distilled prior to use. The other materials were common commercial level and used as received. The molecular structure and synthetic approach of PBDTTID are shown in Scheme 1.

Synthesis of compound (1). Compound (**1**) was synthesized according to the literature procedure.[25]

Synthesis of compound (2). *N*-bromosuccinimide (2.2 g, 12.0 mmol) was added in small portions to a solution of compound (**1**) (1.9 g, 6.0 mmol) in DMF (50 ml) at 0 °C. The reaction mixture was stirred for 1 h at this temperature and then poured into a saturated sodium thiosulphate solution (100 ml). The organic layer was extracted with CH_2Cl_2 and dried over anhydrous $MgSO_4$. After filtration, the solvent was removed under reduced pressure and the residue was purified by flash chromatography on silica gel (eluent: CH_2Cl_2) to yield a yellow powder (2.5 g, 90%). ^{1}H NMR (400 MHz, $CDCl_3$) δ 7.98 (s, 2H), 3.64 (d, J = 6.9 Hz, 2H), 1.97–1.80 (m, 1H), 1.46–1.14 (m, 8H), 1.01–0.75 (m, 6H). ^{13}C NMR (101 MHz, $CDCl_3$) δ 167.45, 138.07, 127.39, 118.57, 110.03, 42.64, 38.28, 30.70, 28.63, 24.06, 23.13, 14.19, 10.57.

Synthesis of compound (3). Compound (**2**) (0.24 g, 0.5 mmol), 2-trimethyl(thiophene-2-yl)stannane (0.56 g, 1.5 mmol), toluene (10 ml) and DMF (2 ml) were mixed in a 50 ml two-neck flask. The reactant was purged with argon for 5 min, and then 20 mg of $Pd(PPh_3)_4$ was added. After being purged for another 20 min, the mixture was allowed to reflux for 16 h and then cool to room temperature. The solvent was removed by rotary evaporation and the crude product was purified by chromatography on silica gel (eluent: from hexane to hexane–CH_2Cl_2 = 1 : 1), to yield a red power (0.23 g, 95%). ^{1}H NMR (400 MHz, $CDCl_3$) δ 8.39 (s, 2H), 7.48 (d, J = 5.0 Hz, 2H), 7.40 (d, J = 3.1 Hz, 2H), 7.23–7.14 (m, 2H), 3.63 (d, J = 7.2 Hz, 2H), 1.95–1.82 (m, 1H), 1.43–1.21 (m, 8H), 0.98–0.83 (m, 6H). ^{13}C NMR (101 MHz, $CDCl_3$) δ 168.04, 135.57, 133.79, 132.60, 128.48, 127.50, 127.37, 126.84, 119.34, 42.47, 38.32, 30.72, 28.68, 24.06, 23.14, 14.22, 10.60.

Synthesis of compound (4). *N*-bromosuccinimide (0.15 g, 0.8 mmol) was dissolved in 5 ml *N*,*N*-dimethylformamide (DMF) and was added dropwise to a solution of compound (**3**) (0.19 g, 0.4 mmol) in 20 ml DMF at 0 °C in the dark. The mixture was stirred for another 1 h at this temperature and then poured into a saturated sodium thiosulphate solution (100 ml). The organic layer was extracted with CH_2Cl_2 and dried over anhydrous $MgSO_4$. After filtration, the solvent was removed under reduced pressure and the residue was purified by flash chromatography on silica gel (eluent: hexane–CH_2Cl_2 = 1 : 1) to yield the monomer as dark red powder (0.33 g, 65%). ^{1}H NMR (400 MHz, $CDCl_3$) δ 8.28 (s, 2H), 7.17–7.10 (m, 4H), 3.62 (d, J = 7.0 Hz, 2H), 1.95–1.80 (m, 1H), 1.47–1.19 (m, 8H), 0.98–0.81 (m, 6H). ^{13}C NMR (101 MHz, $CDCl_3$) δ 167.74, 135.76, 134.97, 131.59, 131.33, 127.67, 127.29, 118.86, 114.61, 42.52, 38.31, 30.71, 28.65, 24.06, 23.13, 14.21, 10.58. $C_{26}H_{23}Br_2NO_2S_3$: Calcd: N 2.20, C 48.99, H 3.64; found: N 2.19, C 48.97, H 3.62%.

Synthesis of the polymer using a Stille coupling reaction. A mixture of compound (**4**) (0.127 g, 0.2 mmol), (4,8-bis((2-hexyldecyl)oxy)benzo[1,2-*b*:4,5-*b*′]dithiophene-2,6-diyl)bis(trimethylstannane) (0.199 g, 0.2 mmol), in toluene (10 ml) and DMF (2 ml) was purged with argon for 30 min, and then 20 mg of $Pd(PPh_3)_4$ was added. After being purged for another 20 min, the mixture was allowed to reflux for 16 h. After cooling to room temperature, the polymer was precipitated in methanol. The crude product was collected by filtration and then purified by washing and extracted on a Soxhlet extractor with methanol and hexane in succession. After that, the polymer was Soxhlet-extracted with chloroform and the chloroform fraction was concentrated by rotary evaporation. The final product was obtained by precipitating the chloroform solution in methanol as a dark blue powder, and drying under vacuum at 40 °C overnight. $(C_{68}H_{93}NO_4S_5)_n$: Calcd: N 1.22, C 71.09, H 8.16; found: N 1.17, C 71.31, H 8.19%.

Characterization

^{1}H and ^{13}C NMR spectra were measured on a Bruker Arx-400 spectrometer. Absorption spectra were taken on a Hitachi U-3010 UV-vis spectrophotometer. The molecular weight of the polymers was measured by the GPC method, and polystyrene was used as a standard using chloroform ($CHCl_3$) as eluent. TGA measurements were performed on a TA Instruments, Inc.

TGA-2050. DSC measurements were performed on a TA Instruments, Inc. DSC-2910. The electrochemical cyclic voltammetry experiments were conducted on a CHI650D Electrochemical Workstation with a glassy carbon disk, Pt wire, and a Ag/Ag^+ electrode as the working electrode, counter electrode, and reference electrode, respectively in a 0.1 mol l^{-1} tetrabutylammonium hexafluorophosphate (Bu_4NPF_6) acetonitrile solution. AFM measurements were performed on a Bruker Veeco MultiMode 8 Atomic Force Microscope, and TEM measurements were performed on Transmission Electron Microscopes (TEM): JEM-2200FS.

Fabrication and characterization of PSCs

Polymer solar cells with device structures of glass/ITO/PEDOT:PSS/Polymer:$PC_{61}BM$/Ca/Al were fabricated as follows: a 30 nm layer of PEDOT:PSS (poly(3,4-ethylenedioxythiophene): poly(styrenesulfonate)) was spin-coated onto pre-cleaned ITO (indium tin oxide) glass substrates, and then the substrates were transferred into a nitrogen filled glovebox. A mixture of polymer–$PC_{61}BM$ in dichlorobenzene was spin-coated as a film on top of the PEDOT:PSS layer. The thickness of the active layer was ~100 nm. The devices were completed by evaporation, and a 20 nm thick layer of Ca and a 80 nm thick layer of Al, with an area of 4 mm^2 as defined by masks, were used as metal electrodes.

Hole mobility measurement

The device was fabricated with the structure ITO/PEDOT:PSS/polymer:$PC_{61}BM$/Au for the hole mobility measurement based on the space-charge-limited current (SCLC) model.

According to the equation:

$$\ln\frac{JL^3}{V^2} = 0.89\left(\frac{1}{E_0}\right)^{0.5}\left(\frac{V}{L}\right)^{0.5} + \left(\frac{9\varepsilon\varepsilon_0\mu_0}{8}\right)$$

where μ_0 is the zero-field mobility, E_0 is the characteristic field, J is the current density, ε is the dielectric constant of the polymer, ε_0 is the permittivity of the vacuum, L is the thickness of the polymer layer, $V = V_{appl} - V_{bi}$, V_{appl} is the applied potential, and V_{bi} is the built-in potential (in this device structure, $V_{bi} = 0.2$ V), the hole mobility can be calculated as 2.34×10^{-5} cm^2 V^{-1} s^{-1}.

Results and discussion

Synthesis and structural characterization

The molecular structure and synthetic approach for PBDTTID are shown in Scheme 1. Compound (**1**) was prepared by the reported method,[25] and the monomer, compound (**4**), was prepared in three steps in good yield. The final product, PBDTTID, was prepared by the Pd-catalyzed Stille coupling reaction between the two monomers using toluene–DMF (5 : 1) as the solvent and $Pd(PPh_3)_4$ as the catalyst. The weight-average molecular weight (M_w) of PBDTTID is 52.3 K with a polydispersity index (PDI) of 2.56, determined by gel permeation chromatography (GPC) using $CHCl_3$ as the eluent. The polymer exhibits good solubility in common solvents, such as $CHCl_3$, chlorobenzene (CB), and dichlorobenzene (DCB). The thermal stability of PBDTTID was investigated by thermogravimetric analysis (TGA). The temperature of the onset point of 5% weight loss (T_d) is around 332 °C. This result indicates that the thermal stability of the copolymer is good enough for application in PSCs. From differential scanning calorimetry (DSC) measurements, we found that no clear glass transition was observed in the range of 0–300 °C under an inert atmosphere. The TGA and DSC plots are shown in the ESI.†

Optical and electrochemical properties

In order to demonstrate the influence of the quinoid effect, a polymer named PBDTTPD (as shown in Scheme 1) was prepared by the method reported by Leclerc *et al.*,[28] and used as a reference material in this work. Fig. 1a shows the ultraviolet-visible (UV-vis) absorption spectra of PBDTTID and PBDTTPD as solid films and in $CHCl_3$ solutions. As shown in Fig. 1a, the absorption edge of the PBDTTPD film is located at 690 nm, corresponding to a band gap of 1.8 eV, and this result is consistent with the reported result.[28] For PBDTTID, the solution shows an absorption peak at 571 nm, and the film exhibits a peak at 630 nm. From the solution state to the solid film, a red shift of *ca.* 50 nm can be observed, and the optical band gap (E_g^{opt}) of PBDTTID is 1.53 eV. Based on these results, it is very clear that after introducing the quinoid structure, the band gap of the polymer can be effectively reduced from 1.80 eV to 1.53 eV.

Electrochemical cyclic voltammetry was employed to measure the molecular energy levels of the material.[29] The cyclic voltammogram (CV) curves of PBDTTID and PBDTTPD are

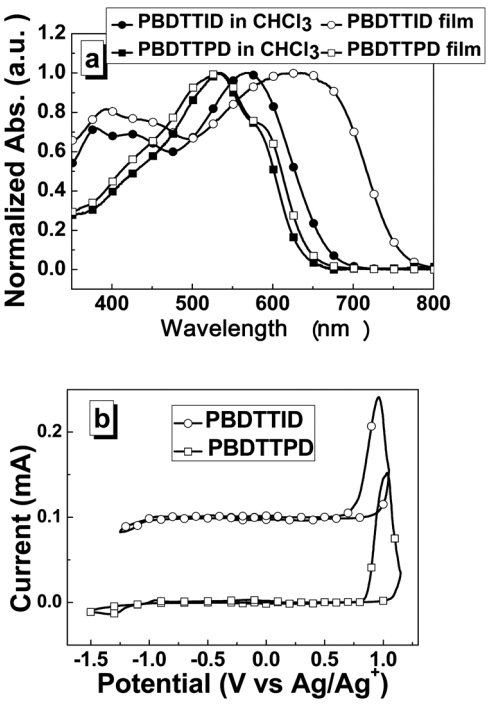

Fig. 1 (a) UV-vis absorption spectra of PBDTTID and PBDTTPD in chloroform solutions and in spin-coated thin films. (b) Cyclic voltammogram of PBDTTID and PBDTTPD drop-cast on glassy carbon, measured in 0.1 M Bu_4NPF_6 at a scan rate of 50 mV s^{-1}.

shown in Fig. 1b. On the basis of the onset potentials, the highest occupied molecular orbital (HOMO) and the lowest unoccupied molecular orbital (LUMO) levels of the control polymer, PBDTTPD, were estimated to be −5.52 eV and −3.70 eV, respectively, which agrees well with reported results.[23] Interestingly, the new polymer PBDTTID exhibits a HOMO level of −5.40 eV, which is 0.12 eV higher than that of PBDTTPD; the LUMO level of PBDTTID is −3.78 eV, which is 0.08 eV lower than that of PBDTTPD.

Comparison of these two polymers indicates that the electrochemical band gap of the polymer can be effectively lowered by introducing the quinoid structure, due to elevation of its HOMO level and reduction of its LUMO level.

It is well known that open circuit voltage (V_{oc}) of a polymer solar cell with bulk-heterojunction structure is closely related to the gap between the HOMO level of the electron donor material and the LUMO level of the electron acceptor material in the blend film,[30,31] and therefore the design of a polymer electron donor material with a deep HOMO level is key to obtaining efficient photovoltaic devices.[32] The low-lying HOMO level and the narrow band gap of PBDTTID indicate that this polymer might be a potential electron donor material in PSCs.

Density functional theory calculations

Density functional theory (DFT) calculations were performed to demonstrate the electronic structures of the two polymers, *e.g.* the HOMO and LUMO surfaces, with a molecular main chain length $n = 3$, at the B3LYP/6-31G level of theory.[33] As shown in Fig. 2, the HOMO surface of PBDTTID is distributed along the conjugated backbone evenly, but its LUMO surface is mainly located at the TID units. For PBDTTPD, both the HOMO and the LUMO surfaces are distributed along the backbone evenly.

Photovoltaic properties

The photovoltaic properties of PBDTTID were investigated by fabricating PSC devices with a ITO/PEDOT:PSS/PBDTTID:$PC_{61}BM$/Ca/Al structure, where PBDTTID was used as the electron donor material and $PC_{61}BM$ was used as the electron acceptor material in the active layer. Different D–A weight ratios, such as 1 : 1, 1 : 2 and 1 : 3 have been scanned to optimize the device performance. Fig. 3a shows the *I–V* curves of the PSC devices based on PBDTTID under illumination of AM 1.5G, 100 mW cm^{-2}, and the corresponding characteristics of the solar cells are summarized in Table 1. The best performance was obtained at a weight ratio of 1 : 1, and a PCE of 1.47% with a V_{oc} of 0.83 V, a short circuit current (J_{sc}) of 3.43 mA cm^{-2} and a fill factor (FF) of 0.52 were recorded. Moreover, the photovoltaic performance of the PSC device can be further improved by using 3% (v/v) diiodooctane (DIO) as a solvent additive.[34] After being processed with DIO, the device's J_{sc} significantly increased from 3.43 mA cm^{-2} to 6.5 mA cm^{-2}. As a result, the PCE increased to 3.12%. To make a clear comparison, PSC devices based on the analogue copolymer PBDTTPD were fabricated and tested under the same conditions, and the results are listed in Table 1. The PBDTTPD-based device exhibits a PCE of 0.92%, and the V_{oc}, J_{sc} and FF are 0.87 V, 2.35 mA cm^{-2} and 0.45, respectively. It is obvious that the PBDTTID-based device exhibits a slightly lower V_{oc}, but better J_{sc} and FF compared to the PBDTTPD-based device. Moreover, the hole mobility of the active layer of the best device was measured by the space-charge-limited current (SCLC) method,[35] and the hole mobility can be estimated to be 2.34×10^{-5} cm^2 V^{-1} s^{-1}.

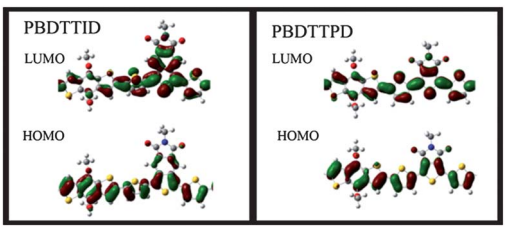

Fig. 2 The frontier molecular orbitals of PBDTTID (left) and PBDTTPD (right) obtained from DFT calculations.

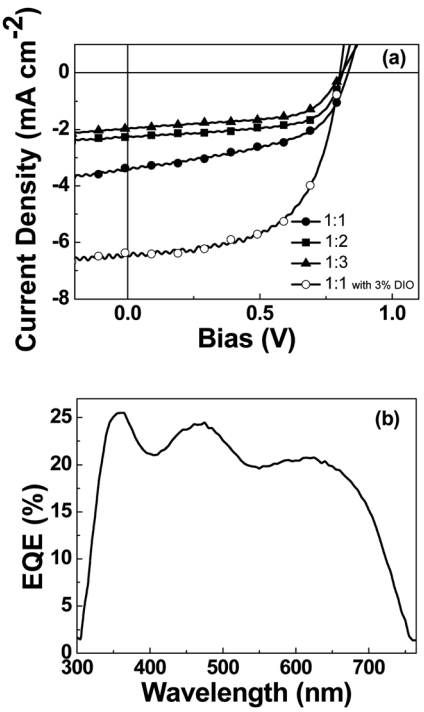

Fig. 3 (a) *I–V* curves of the PSC devices based on PBDTTID under illumination of AM 1.5G, 100 mW cm^{-2}. (b) EQE curve of the photovoltaic cells with polymer:$PC_{61}BM$ = 1 : 1 with 3% (v/v) DIO as additive as the active layer.

Table 1 Photovoltaic results of solar cells based on PBDTTID:$PC_{61}BM$ and PBDTTPD:$PC_{61}BM$

Polymer	D : A (w/w)	J_{sc} (mA cm^{-2})	V_{oc} (V)	FF (%)	PCE (%)
PBDTTID	1 : 1	3.43	0.83	0.52	1.47
	1 : 2	2.30	0.81	0.63	1.17
	1 : 3	1.99	0.81	0.59	0.96
	1 : 1[a]	6.50	0.80	0.60	3.12
PBDTTPD	1 : 1	2.35	0.87	0.45	0.92

[a] 3% DIO additive (v/v).

Fig. 3b shows the external quantum efficiency (EQE) curve of the PSC device with optimal photovoltaic performance. The integral current density based on the EQE curve is ~6.3 mA cm^{-2}, which is consistent with the result from the *I–V* measurement. It can be seen that the response range of the device covers almost the whole visible wavelength range from 300 nm to 750 nm, but the peak value of EQE is only 25%. It is obvious that the photovoltaic performance of the PBDTTID-based device is limited by the low EQE.

From the device results, it was found that using DIO as a solvent additive plays an important role in improving the photovoltaic performance of the devices. According to the reported works, appropriate phase separation is necessary to form bicontinuous channels which facilitate charge transport in the donor–acceptor blend. Therefore, atomic force microscopy (AFM) and transmission electron microscopy (TEM) were used to reveal the morphology of the PBDTTID/$PC_{61}BM$ blend films prepared with and without DIO. The AFM and TEM images are shown in Fig. 4. It is clear that, compared with the blend film prepared from DCB solution without using DIO as a solvent additive, after using DIO, a smaller domain size can be observed, *e.g.* ~20 nm for a nanoscale structure. This morphology is favourable for efficient exciton dissociation and charge transport, resulting in a higher PCE,[36] and this phenomenon is consistent with reported works.[9,37]

Conclusions

In conclusion, a new photovoltaic polymer with strong quinoid properties, PBDTTID, was designed and synthesized. The polymer exhibits good solubility in common solvents and good thermal stability below 332 °C. UV-vis measurements indicated the polymer thin film exhibited broad absorption in the region from 300 nm to 800 nm, and the HOMO and LUMO energy levels of the polymer are −5.40 eV and −3.78 eV, respectively, estimated from electrochemical cyclic voltammetry measurements. The electronic structures of the of the two polymers were also studied by DFT calculations at the B3LYP/6-31G level. Compared to PBDTTPD, the counterpart of PBDTTID, the influence of the quinoid structure on the polymer's properties can be clearly seen. By introducing the quinoid unit, the HOMO level of the polymer is elevated and the LUMO level is lowered, and consequently the band gap of the polymer can be reduced very effectively. The PBDTTID-based PSC device shows a slightly lower V_{oc} but better J_{sc} and FF than the PBDTTPD-based PSC device. Considering that the former shows much broader response range than the latter, it can be concluded the introduction of the quinoid structure has a very positive effect on the photovoltaic properties of the polymer. Since the preliminary polymer, PBDTTID, exhibits some promising photovoltaic properties, like high V_{oc}, good FF and a broad response range, it might be a potential photovoltaic polymer. Furthermore, TID will be a desirable building block towards the design of photovoltaic polymers with a low-lying HOMO level as well as a low band gap.

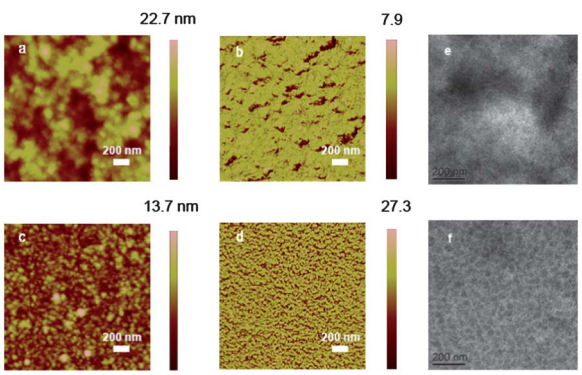

Fig. 4 Tapping mode AFM (a–d) and TEM (e, f) images of PBDTTID/$PC_{61}BM$ films prepared by spin-coating from a 1,2-DCB solution with (a, b, e) and without (c, d, f) DIO (3%, v/v).

Acknowledgements

This work was supported by the National High-tech R&D Program of China (863 Program, no. 2011AA050523) and the National Natural Science Foundation of China (NSFC, no. 51173189).

References

1 G. Yu, J. Gao, J. C. Hummelen, F. Wudl and A. J. Heeger, *Science*, 1995, **270**, 1789–1791.
2 G. Dennler, M. C. Scharber and C. J. Brabec, *Adv. Mater.*, 2009, **21**, 1323–1338.
3 L. Huo, S. Zhang, X. Guo, F. Xu, Y. Li and J. Hou, *Angew. Chem., Int. Ed.*, 2011, **50**, 9697–9702.
4 H.-Y. Chen, J. Hou, S. Zhang, Y. Liang, G. Yang, Y. Yang, L. Yu, Y. Wu and G. Li, *Nat. Photonics*, 2009, **3**, 649–653.
5 H. Zhou, L. Yang, A. C. Stuart, S. C. Price, S. Liu and W. You, *Angew. Chem., Int. Ed.*, 2011, **50**, 2995–2998.
6 J. M. Szarko, J. Guo, Y. Liang, B. Lee, B. S. Rolczynski, J. Strzalka, T. Xu, S. Loser, T. J. Marks, L. Yu and L. X. Chen, *Adv. Mater.*, 2010, **22**, 5468–5472.
7 S. C. Price, A. C. Stuart, L. Yang, H. Zhou and W. You, *J. Am. Chem. Soc.*, 2011, **133**, 4625–4631.
8 Z. He, C. Zhong, X. Huang, W.-Y. Wong, H. Wu, L. Chen, S. Su and Y. Cao, *Adv. Mater.*, 2011, **23**, 4636–4643.
9 Y. Liang, Z. Xu, J. Xia, S.-T. Tsai, Y. Wu, G. Li, C. Ray and L. Yu, *Adv. Mater.*, 2010, **22**, E135–E138.
10 L. Dou, J. You, J. Yang, C.-C. Chen, Y. He, S. Murase, T. Moriarty, K. Emery, G. Li and Y. Yang, *Nat. Photonics*, 2012, **6**, 180–185.
11 T. Yang, M. Wang, C. Duan, X. Hu, L. Huang, J. Peng, F. Huang and X. Gong, *Energy Environ. Sci.*, 2012, **5**, 8208–8214.
12 T.-Y. Chu, J. Lu, S. Beaupre, Y. Zhang, J.-R. Pouliot, S. Wakim, J. Zhou, M. Leclerc, Z. Li, J. Ding and Y. Tao, *J. Am. Chem. Soc.*, 2011, **133**, 4250–4253.
13 Z. Tan, W. Zhang, Z. Zhang, D. Qian, Y. Huang, J. Hou and Y. Li, *Adv. Mater.*, 2012, **24**, 1476–1481.
14 E. E. Havinga, W. ten Hoeve and H. Wynberg, *Synth. Met.*, 1993, **55**, 299–306.

15 S. H. Park, A. Roy, S. Beaupre, S. Cho, N. Coates, J. S. Moon, D. Moses, M. Leclerc, K. Lee and A. J. Heeger, *Nat. Photonics*, 2009, **3**, 297–302.
16 J. Hou, H.-Y. Chen, S. Zhang, G. Li and Y. Yang, *J. Am. Chem. Soc.*, 2008, **130**, 16144–16145.
17 N. Blouin, A. Michaud and M. Leclerc, *Adv. Mater.*, 2007, **19**, 2295–2300.
18 M. Chen, J. Hou, Z. Hong, G. Yang, S. Sista, L. Chen and Y. Yang, *Adv. Mater.*, 2009, **21**, 4238–4242.
19 E. Zhou, M. Nakamura, T. Nishizawa, Y. Zhang, Q. Wei, K. Tajima, C. Yang and K. Hashimoto, *Macromolecules*, 2008, **41**, 8302–8305.
20 J. Chen and Y. Cao, *Acc. Chem. Res.*, 2009, **42**, 1709–1718.
21 J. Hou, H.-Y. Chen, S. Zhang, R. I. Chen, Y. Yang, Y. Wu and G. Li, *J. Am. Chem. Soc.*, 2009, **131**, 15586–15587.
22 Y. Liang, D. Feng, Y. Wu, S.-T. Tsai, G. Li, C. Ray and L. Yu, *J. Am. Chem. Soc.*, 2009, **131**, 7792–7799.
23 J. Hou, M.-H. Park, S. Zhang, Y. Yao, L.-M. Chen, J.-H. Li and Y. Yang, *Macromolecules*, 2008, **41**, 6012–6018.
24 Y. Zhu, R. D. Champion and S. A. Jenekhe, *Macromolecules*, 2006, **39**, 8712–8719.
25 H. Meng and F. Wudl, *Macromolecules*, 2001, **34**, 1810–1816.
26 H. Li, S. Sun, T. Salim, S. Bomma, A. C. Grimsdale and Y. M. Lam, *J. Polym. Sci., Part A: Polym. Chem.*, 2012, **50**, 250–260.
27 W. A. Braunecker, Z. R. Owczarczyk, A. Garcia, N. Kopidakis, R. E. Larsen, S. R. Hammond, D. S. Ginley and D. C. Olson, *Chem. Mater.*, 2012, **24**, 1346–1356.
28 A. Najari, S. Beaupre, P. Berrouard, Y. Zou, J.-R. Pouliot, C. Lepage-Perusse and M. Leclerc, *Adv. Funct. Mater.*, 2011, **21**, 718–728.
29 Y. Li, Y. Cao, J. Gao, D. Wang, G. Yu and A. J. Heeger, *Synth. Met.*, 1999, **99**, 243–248.
30 M. C. Scharber, D. Mühlbacher, M. Koppe, P. Denk, C. Waldauf, A. J. Heeger and C. J. Brabec, *Adv. Mater.*, 2006, **18**, 789–794.
31 G. Dennler, M. C. Scharber and C. J. Brabec, *Adv. Mater.*, 2009, **21**, 1323–1338.
32 L. Huo, X. Guo, Y. Li and J. Hou, *Chem. Commun.*, 2011, **47**, 8850–8852.
33 R. G. Parr and Y. Weitao, *Density Functional Theory of Atoms and Molecules*, Oxford University Press, New York, 1989.
34 J. Peet, J. Kim, N. Coates, W. Ma, D. Moses, A. Heeger and G. Bazan, *Nat. Mater.*, 2007, **6**, 497–500.
35 J. Hou, C. Yang, J. Qiao and Y. Li, *Synth. Met.*, 2005, **150**, 297–304.
36 G. Li, V. Shrotriya, Y. Yao, J. Huang and Y. Yang, *J. Mater. Chem.*, 2007, **17**, 3126–3140.
37 C. M. Amb, S. Chen, K. R. Graham, J. Subbiah, C. E. Small, F. So and J. R. Reynolds, *J. Am. Chem. Soc.*, 2011, **133**, 10062–10065.